Supplemental Figure 1:
Temporal and spatial deposition and removal of fibrin during fracture repair.
Displaced transverse femur fractures we examine by radiography, Safranin-O, angiography, and fibrin-immunofluorescence microscopy. One day post fracture (1-DPF) the cortex is disrupted (yellow arrow-radiographs and Safranin-O) with a concomitant disruption of the vasculature resulting in an avascular

segment of bone proximal and distal to the fracture site (angiogram). Fibrin is observed in abundance both within the intramedullary space and soft tissues adjacent to the fracture site (Fibrin). By 10-DPF, an avascular soft-tissue callus forms directly around the fracture site (Safranin-O and angiogram) and a hard-tissue callus initiates at the proximal and distal aspects of the soft tissue callus (blue arrowheads - radiographs). Note that during this early stage of fracture healing there is a marked reduction in fibrin deposition in the soft-tissues surrounding the fracture site (Fibrin), while intramedullary fibrin persists (10-DPF). As the endochondral-mediated vascularization (angiogram) and associated hard-tissue callus (radiographs) replaces the soft-tissue callus (14-DPF), fibrin is notably absent from the fracture callus and intramedullary space (Fibrin). White box denotes area of 20x fibrin. Scale bars = 1-mm. Representative of n≥3 for each analysis.

Supplemental Figure 2:

Predicted torsional strength and rigidity of hard tissue callus by *μ*CT-derived finite element analysis.

Using a computational method sensitive to the contribution of structure to stiffness and strength of an object, predicted callus strength and rigidity did not significantly (Mann-Whitney T-test) differ between WT and $Fbg^{-/-}$ mice. Error bars = SD, n=7 per genotype.

Supplemental Figure 3:

Antisense Oligonucleotide Knock down of Fibrinogen in Plasma.

To ensure knockdown of fibrinogen in $Plg^{-/-}$ mice prior to fracture we conducted a pilot study. $Plg^{-/-}$ mice were treated with fibrinogen ASO for 2 weeks and then sacrificed. mRNA data demonstrates a dose dependent knock down of fibrinogen (Top) ** $P<0.01$ by Mann-Whitney T-test. Values shown are relative to control. Reduction in circulating fibrinogen was confirmed by ELISA (bottom). Note that $Plg^{-/-}$ mice administered 100mg/kg per week (mpk/wk) fibrinogen ASO had no detectable circulating fibrinogen. Error bars = SEM

Supplemental Figure 4:

Radiographic Assessment of Fracture Repair

Quantification of fracture repair using a radiographic scoring method. Note no significant differences in the radiographic scoring between WT and $Fbg^{-/-}$ mice whereas the data reveal significant impairment of fracture repair in $Plg^{-/-}$ mice. Reduction of fibrinogen in $Plg^{-/-}$ mice ($Plg^{-/-}Fbg^{low}$) partially rescued $Plg^{-/-}$ induced deficits in fracture repair. Additionally, note no difference in fracture repair between Plg-/- and Plg-/-control mice. Fracture repair scores were determined from serial radiographs (see Methods) form WT (n=15), $Fbg^{-/-}$ (n=10), Plg-/- (n=15) Plg-/-control (n=5) and $Plg^{-/-}Fbg^{Low}$ (n=13) mice were recorded weekly. Data displayed represent the mean ± SD. Statistical significance was determined using a two-way ANOVA. (*** = $P<0.001$ $Plg^{-/-}$ Fbg^{low} compared to $Plg^{-/-}$ mice; ††† = $P<0$ .001 $Plg^{-/-}$ Fbg^{low} compared to WT mice, §§§ = $P<0$ .001 $Plg^{-/-}$ mice compared to WT mice).

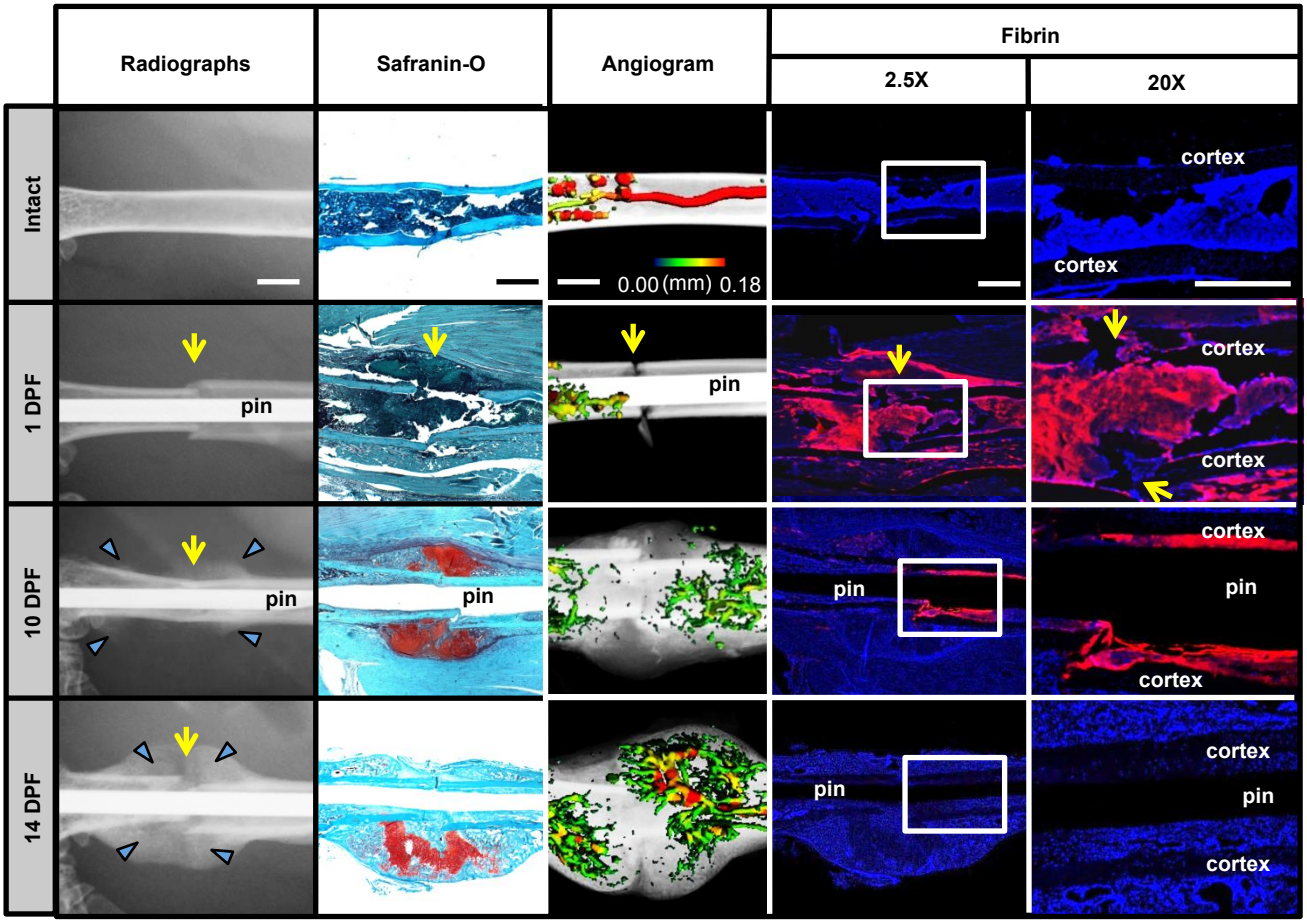

Supplementary Figure 1

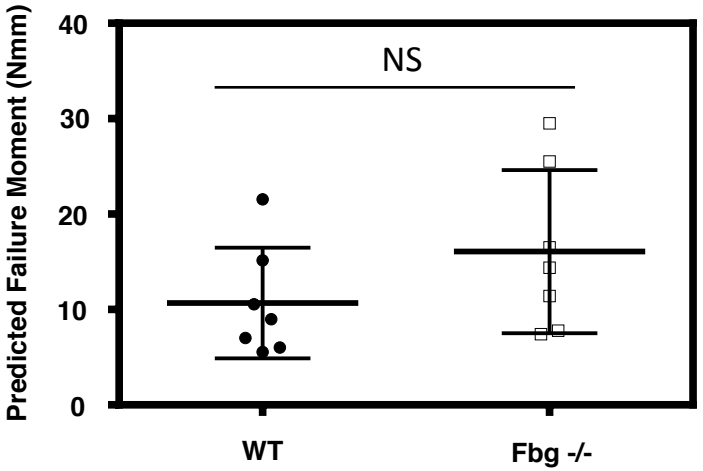

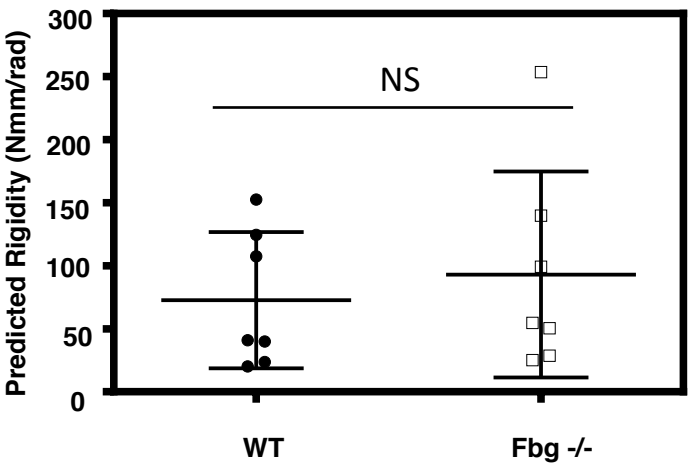

Supplementary Figure 2

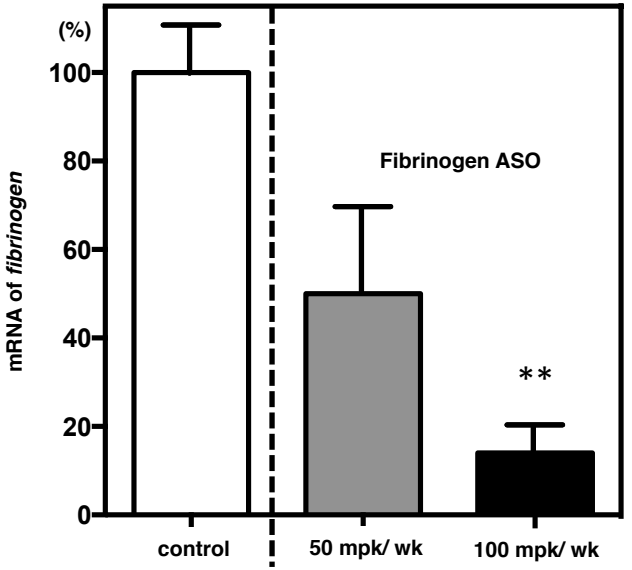

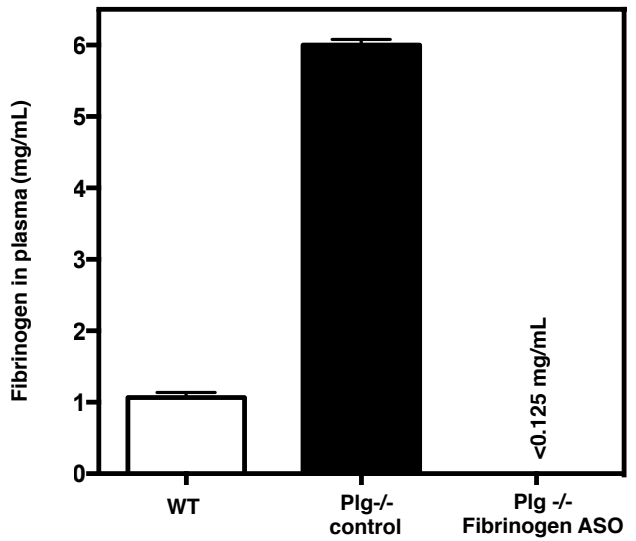

Supplementary Figure 3

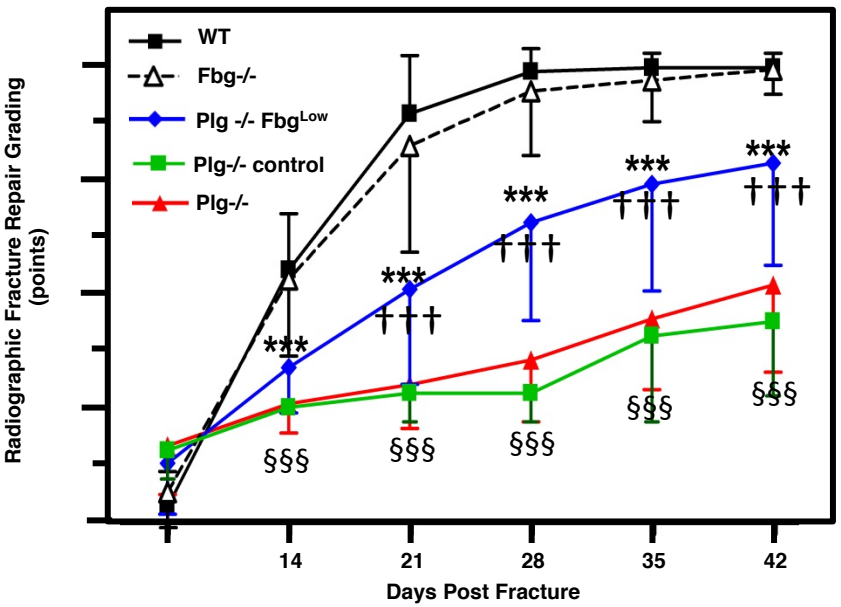

Supplementary Figure 4